

# Hydrogen-bonded Organo-amino Phosphonium Halides: Dielectric, Piezoelectric and Possible Ferroelectric Properties

Thangavel Vijayakanth,<sup>a</sup> Richa Pandey,<sup>c</sup> Priyangi Kulkarni,<sup>e</sup> Balu Praveenkumar<sup>\*e</sup>, Dinesh Kabra<sup>\*d</sup> and Ramamoorthy Boomishankar<sup>\*a,b</sup>

<sup>a</sup>Department of Chemistry and <sup>b</sup>Centre for Energy Science, Indian Institute of Science Education and Research (IISER) Pune, Dr. Homi Bhabha Road, Pune, India – 411008.

E-mail: [boomi@iiserpune.ac.in](mailto:boomi@iiserpune.ac.in)

<sup>c</sup>Centre for Research in Nanotechnology, Indian Institute of Technology, Bombay, Powai, Mumbai 400076.

<sup>d</sup>Department of Physics, Indian Institute of Technology, Bombay, Powai, Mumbai 400076.

E-mail: [dkabra@phy.iitb.ac.in](mailto:dkabra@phy.iitb.ac.in)

<sup>d</sup>PZT Centre, Armament Research and Development Establishment (ARDE), Defence Research and Development Organization (DRDO), Dr. Homi Bhabha Road, Pune, India – 411008.

E-mail: [praveenkumar@arde.drdo.in](mailto:praveenkumar@arde.drdo.in)

## Supporting Information

S.N.	Table of Contents	Page No.
1	Experimental Section	2-3
2	Crystallographic Information	4-7
3	Characterization Data	8-16
4	Ferroelectric, PFM and Dielectric studies	17-25
5	Comparison of Piezoelectric Materials	26
6	References	27

## EXPERIMENTAL SECTION

### General Remarks

All the manipulations involving phosphorous halides were carried out under dry nitrogen conditions in standard Schlenk glassware. The dichloromethane ( $\text{CH}_2\text{Cl}_2$ ) solvent was dried over phosphorous pentaoxide ( $\text{P}_2\text{O}_5$ ). Diphenylchlorophosphine ( $\text{Ph}_2\text{PCl}$ ), isopropylamine, liquid bromine ( $\text{Br}_2$ ) Sodium chloride ( $\text{NaCl}$ ) and Sodium iodide ( $\text{NaI}$ ) were purchased from Sigma Aldrich and used as received. The NMR spectra were recorded in deuterated chloroform ( $\text{CDCl}_3$ ) on a Bruker 400 MHz spectrometer ( $^1\text{H}$  NMR, 400.13 MHz;  $^{13}\text{C}$  { $^1\text{H}$ } NMR, 100.62 MHz;  $^{31}\text{P}$  { $^1\text{H}$ } NMR, 161.97 MHz, at room temperature using  $\text{SiMe}_4$  ( $^1\text{H}$ ,  $^{13}\text{C}$ ) and 85%  $\text{H}_3\text{PO}_4$  ( $^{31}\text{P}$ ) as standards. The ESI and MALDI-TOF spectra were obtained by using Waters Synapt G2 and the Applied Biosystem MALDI-TOF/TOF spectrometers, respectively. FT-IR spectrum was performed on a Perkin-Elmer spectrometer with samples prepared as KBr pellets. The variable temperature powder X-ray diffraction data were measured in the 2-theta range of 5° to 50° on a Bruker-D8 Advance X-ray diffractometer. The thermogravimetric analysis was performed by using the PerkinElmer STA-6000 analyzer with a heating rate of 10 °C/min in a nitrogen atmosphere. Melting point analyses were performed by using Electro thermal melting point apparatus and were uncorrected.

### Synthesis of diphenyl diisopropylaminophosphonium halides DPDP-X (X = Cl, Br, I):

**DPDP-Br:** The starting compound of DPDP-Br was synthesized by our earlier reported procedure.<sup>1</sup>

**DPDP-Cl:** To a stirred solution of DPDP-Br (1 g, 0.0026 mol) in methanol (20 mL), NaCl (0.46 g, 0.0078 mol) in water (10 mL) was slowly added with the formation of NaBr precipitate. The reaction mixture was stirred at room temperature for a further period of 10-15 min. and filtered through celite. The obtained clear solution was left out for the crystallization. Colorless plate like crystals of DPDP-Cl were obtained after one week. Yield: 0.85 g (97%). M.P. 224-229°C.  $^1\text{H}$  NMR (400 MHz,  $\text{CDCl}_3$ ) δ 8.05 – 7.97 (m, 4H), 7.62 – 7.55 (m, 2H), 7.50 – 7.45 (m, 4H), 6.75 – 6.69 (m, 2H), 3.37 – 3.25 (m, 2H), 1.20 (d,  $J$  = 6.5 Hz, 12H).  $^{13}\text{C}$  NMR (100 MHz,  $\text{CDCl}_3$ ) δ 133.87, 133.15, 129.35, 125.34, 44.65, 24.80.  $^{31}\text{P}$  NMR (162 MHz,  $\text{CDCl}_3$ ): δ 34.74 ppm. FT-IR data in KBr pellet ( $\text{cm}^{-1}$ ): 3141, 2967, 2882, 2729, 1591, 1426, 1312, 1161, 1075, 1020, 919, 892, 832, 751, 726, 699 and 615. MALDI-TOF = 301.1828 [M $^+$ ]. Anal. Calcd. For  $\text{C}_{18}\text{H}_{26}\text{ClN}_2\text{P}$ : C 64.18; H 7.78; N 8.32. Found: C 64.11; H 7.71; N 8.30.

**DPDP-I:** To a stirred solution of DPDP-Br (1 g, 0.0026 mol) in any one of the solvent systems such as MeOH, MeOH/H<sub>2</sub>O, MeCN, MeCN/H<sub>2</sub>O, MeCN/MeOH, (20 mL), NaI (1.17 g, 0.0078 mol) in water (10 mL) was slowly added with the formation of NaBr precipitate. The reaction mixture was stirred at room temperature for a further period of 10-15 min. And filtered through celite. The obtained clear solution was left out for the crystallization. Colourless crystals of any one of the two polymorphic phase of DPDP-I (PM1) or DPDP-I (PM2) were obtained after seven days.

**Polymorph DPDP-I (PM1):** M.P. 203-207 °C.  $^1\text{H}$  NMR (400 MHz,  $\text{CDCl}_3$ ) δ 7.99 – 7.93 (m, 4H), 7.70 – 7.65 (m, 2H), 7.59 – 7.54 (m, 4H), 5.39 – 5.33 (m, 2H), 3.50 – 3.38 (m, 2H), 1.28 (d,  $J$  = 6.5 Hz, 12H).  $^{13}\text{C}$  NMR (100 MHz,  $\text{CDCl}_3$ ) δ 134.52, 133.18, 129.69, 124.05, 45.25, 25.06.  $^{31}\text{P}$  NMR (162 MHz,  $\text{CDCl}_3$ ): δ 35.40 ppm. FT-IR data in KBr pellet ( $\text{cm}^{-1}$ ): 3142, 2973, 2935, 1584, 1422, 1315, 1165, 1056, 1020, 915, 899, 832, 754, 725, 693, and 624. MALDI-TOF = 301.1828 [M $^+$ ]. Anal. Calcd. For  $\text{C}_{18}\text{H}_{26}\text{IN}_2\text{P}$ : C 50.48; H 6.12; N 6.54. Found: C 50.45; H 6.10; N 6.53.

**Polymorph DPDP-I (PM2):** M.P. 203-205 °C.  $^1\text{H}$  NMR (400 MHz,  $\text{CDCl}_3$ ) δ 8.01 – 7.94 (m, 4H), 7.67 – 7.63 (m, 2H), 7.57 – 7.52 (m, 4H), 5.52 – 5.47 (m, 2H), 3.52 – 3.41 (m, 2H), 1.28 (d,  $J$  = 6.5 Hz, 12H).  $^{13}\text{C}$  NMR (100 MHz,  $\text{CDCl}_3$ ) δ 134.43, 133.25, 129.62, 124.13, 45.21, 25.06.  $^{31}\text{P}$  NMR (162 MHz,  $\text{CDCl}_3$ ): δ 35.12 ppm. FT-IR data in KBr pellet ( $\text{cm}^{-1}$ ): 3127, 2967, 2929, 1590, 1436, 1308, 1161, 1053, 1019, 916, 890, 830, 754, 726, 690, and 624. MALDI-TOF = 301.1828 [M $^+$ ]. Anal. Calcd. For  $\text{C}_{18}\text{H}_{26}\text{IN}_2\text{P}$ : C 50.48; H 6.12; N 6.54. Found: C 50.45; H 6.10; N 6.53.

### Ferroelectric, Dielectric and Piezoelectric Measurements

The temperature dependent ferroelectric measurements were performed on the single crystals of DPDP-Br, DPDP-Cl and DPDP-I (PM1 & PM2) using a Sawyer-Tower circuit at an operating frequency of 20 to 50 Hz. The single crystal of these organo amino phosphonium salts were deposited with a conducting silver paste prior to the measurements. The polarization (P) vs. Electric Field (E) measurements were performed on an aixACCT TF-2000E model hysteresis loop analyzer. Further the electric field dependent dielectric polarizations of these samples were performed on their single crystals of DPDP-Br, DPDP-Cl and DPDP-I (PM1 & PM2) by keeping the frequency constant at different voltages. The temperature and frequency dependent dielectric constants were measured in a Novocontrol Dielectric Spectrometer. The frequency dependent dielectric polarizations of all the phosphonium halides were performed on their single crystals between 100 Hz and 1 MHz by using LCR meter. The observed capacitance value of these salts further converted into dielectric constant. The  $d_{33}$  measurements were performed on a Piezotest meter model PM300 on the single crystals of DPDP-Br, DPDP-Cl and DPDP-I (PM1 & PM2).<sup>4</sup> The theoretical dipole moment of the all the phosphonium salts was calculated by using Gaussian 09 program. The phosphonium cation assigned as a lower layer and anionic part as selected high layer to perform the ONIOM calculation. The dipole moment calculations were performed by using the DFT methods.<sup>5</sup>

### Second Harmonic Generation (SHG) Measurements

The second harmonic generation (SHG) analysis of all the synthesized phosphonium salts was measured by using Kurtz and Perry method. The irradiation frequency of 1064 nm was generated by using Q-switched Nd:YAG laser. For the SHG measurements, the unsieved powders of the sample obtained from the ground single crystals were filled into a capillary tube, and powdered KDP sample was used as a reference. The intensities of the output emitted from the samples were detected by a photomultiplier tube. The particle sizes of all the compounds were identified by performing Zeiss Ultra Plus field emission scanning electron microscopy (FESEM) which approximately gave the particle sizes to be 1-10  $\mu\text{m}$ .

### Piezoresponse Force Microscopy (PFM) Measurements

In PFM study, the alternating current (AC) voltage is kept constant at 2.5 V and the applied external electric field from the metal (Pt-Ir) coated conductive tip is perpendicular to the as prepared thin film of samples. For this study, the thin films of DPDP-Br, DPDP-Cl and DPDP-I (PM1 & PM2) samples were spin coated on the ITO/Glass substrate and annealed at 120°C. The polarization switching and local piezoelectric responses of all the thin film samples were studied at room temperature with an Asylum Research MFP-3D atomic force microscope working in contact mode. An ASYLEC-01 cantilever made of a tetrahedral silicon tip coated with titanium / Iridium (5/20) was used to apply a small A.C. voltage with an amplitude of 2.5 V. Measurements were performed by applying two oscillating voltages with frequencies below and above resonance (320 kHz), operating the cantilever in the dual a.c. resonance tracking mode.

### Single-crystal X-ray Diffraction Analysis

Single crystal X-ray diffraction data for DPDP·Br, DPDP·Cl, and DPDP·I (PM1 & PM2), at various temperatures were obtained on a Bruker Smart Apex Duo diffractometer by using Mo K $\alpha$  radiation ( $\lambda = 0.71073\text{\AA}$ ). The structures were solved by intrinsic or direct methods and then refined by full-matrix least squares against F<sup>2</sup> using all data by using SHELXL-2014/7 built in the Apex 3 program.<sup>2</sup> Crystallographic refinement data for these compounds are listed in Table S1. All the non-hydrogen atoms were refined anisotropically. Hydrogen atoms were constructed in geometric positions to their parent atoms.<sup>3</sup> The bond distances and angles and structural illustrations were obtained by using the DIAMOND-3.1 software package.

**Table S1.** Single crystal X-ray crystallographic data collection of phosphonium compounds at different temperatures

Compound	DPDP·Cl	DPDP·Cl
Chemical formula	C <sub>18</sub> H <sub>26</sub> CIN <sub>2</sub> P	C <sub>18</sub> H <sub>26</sub> CIN <sub>2</sub> P
Formula weight	336.83	336.83
Temperature	100(2)K	373(2)K
Crystal system	Orthorhombic	Orthorhombic
Space group	Pna <sub>2</sub> <sub>1</sub>	Pna <sub>2</sub> <sub>1</sub>
a (Å); $\alpha$ (°)	14.820(3) : 90	14.976(8) : 90
b (Å); $\beta$ (°)	13.479(3) : 90	13.602(6) : 90
c (Å); $\gamma$ (°)	9.4805(17) : 90	9.504(5) : 90
V (Å <sup>3</sup> ); Z	1893.8(6) : 4	1936.0(17) : 4
$\rho$ (calc.) mg m <sup>-3</sup>	1.181	1.156
$\mu$ (Mo K $\alpha$ ) mm <sup>-1</sup>	0.285	0.279
2 $\theta$ <sub>max</sub> (°)	55.76	55.74
R(int)	0.0630	0.0560
Completeness to $\theta$	100	100
Data / param.	4521/ 175	3856/ 175
GOF	1.041	1.021
R1 [F>4 $\sigma$ (F)]	0.0414	0.0414
wR2 (all data)	0.1175	0.1177
max. peak/hole (e.Å <sup>-3</sup> )	0.706/-0.382	0.354/-0.156
Compound	DPDP·Br	DPDP·Br
Chemical formula	C <sub>18</sub> H <sub>26</sub> BrN <sub>2</sub> P	C <sub>18</sub> H <sub>26</sub> BrN <sub>2</sub> P
Formula weight	381.29	381.29
Temperature	100(2)K	373(2)K
Crystal system	Orthorhombic	Orthorhombic
Space group	Pna <sub>2</sub> <sub>1</sub>	Pna <sub>2</sub> <sub>1</sub>
a (Å); $\alpha$ (°)	14.851(4) : 90	14.966(6) : 90
b (Å); $\beta$ (°)	13.856(3) : 90	13.906(6) : 90
c (Å); $\gamma$ (°)	9.599(2) : 90	9.583(4) : 90
V (Å <sup>3</sup> ); Z	1975.3(8) : 4	1994.4(15) : 4
$\rho$ (calc.) mg m <sup>-3</sup>	1.282	1.270
$\mu$ (Mo K $\alpha$ ) mm <sup>-1</sup>	2.161	2.141
2 $\theta$ <sub>max</sub> (°)	55.75	54.96
R(int)	0.0324	0.0767
Completeness to $\theta$	100	100
Data / param.	4082/ 175	4102/ 175
GOF	1.071	1.029
R1 [F>4 $\sigma$ (F)]	0.0198	0.0461
wR2 (all data)	0.0513	0.1303
max. peak/hole (e.Å <sup>-3</sup> )	0.321/-0.438	0.448/-0.479

<b>Compound</b>	<b>DPDP-I (PM1)</b>	<b>DPDP-I (PM1)</b>
Chemical formula	C <sub>18</sub> H <sub>26</sub> IN <sub>2</sub> P	C <sub>18</sub> H <sub>26</sub> IN <sub>2</sub> P
Formula weight	428.28	428.28
Temperature	100(2)K	373(2)K
Crystal system	Monoclinic	Monoclinic
Space group	Cc	Cc
a (Å); α (°)	15.2497(15) : 90	15.3375(17) : 90
b (Å); β(°)	9.0129(9) : 102.343(2)	9.1435(10) : 102.476(3)
c (Å); γ (°)	14.6473(15) : 90	14.7606(17) : 90
V (Å <sup>3</sup> ); Z	1966.6(3) : 4	2021.1(4) : 4
ρ (calc.) mg m <sup>-3</sup>	1.446	1.407
μ(Mo K <sub>α</sub> ) mm <sup>-1</sup>	1.709	1.663
2θ <sub>max</sub> (°)	56.58	55.74
R(int)	0.0330	0.0532
Completeness to θ	100	100
Data / param.	4451/ 175	3927/ 175
GOF	1.068	1.042
R1 [F>4σ(F)]	0.0194	0.0385
wR2 (all data)	0.0426	0.1000
max. peak/hole (e.Å <sup>-3</sup> )	0.370/-0.579	0.861/-0.721
<b>Compound</b>	<b>DPDP-I (PM2)</b>	<b>DPDP-I (PM2)</b>
Chemical formula	C <sub>18</sub> H <sub>26</sub> IN <sub>2</sub> P	C <sub>18</sub> H <sub>26</sub> IN <sub>2</sub> P
Formula weight	428.28	428.28
Temperature	100(2)K	373(2)K
Crystal system	Monoclinic	Monoclinic
Space group	P2 <sub>1</sub>	P2 <sub>1</sub>
a (Å); α (°)	9.602(10) : 90	9.6471(13) : 90
b (Å); β(°)	15.137(15) : 92.026(19)	15.345(2) : 92.161(3)
c (Å); γ (°)	13.562(15) : 90	13.770(2) : 90
V (Å <sup>3</sup> ); Z	1970.(4) : 4	2037.0(5) : 4
ρ (calc.) mg m <sup>-3</sup>	1.444	1.396
μ(Mo K <sub>α</sub> ) mm <sup>-1</sup>	1.706	1.650
2θ <sub>max</sub> (°)	53.46	54.96
R(int)	0.0600	0.0701
Completeness to θ	100	100
Data / param.	8349/349	8293/357
GOF	1.011	1.020
R1 [F>4σ(F)]	0.0279	0.0432
wR2 (all data)	0.0595	0.1063
max. peak/hole (e.Å <sup>-3</sup> )	0.304/-0.398	0.525/-0.638

**Table S2.** Selected bond lengths [Å] and angles [°] for DPDP·Cl, DPDP·Br and DPDP·I (PM1 & PM2)

Compound	Bond length	Bond angle
<b>DPDP·Cl</b>	P(1)-N(1) : 1.613(3) P(1)-N(2) : 1.618(3) N(1)-H(1) : 0.8800(1) N(2)-H(2) : 0.8800(1)	N(1)-P(1)-N(2) : 109.56(15) N(1)-P(1)-C(11) : 108.56(12) N(1)-P(1)-C(21) : 111.54(14) N(2)-P(1)-C(11) : 113.50(13) N(2)-P(1)-C(21) : 106.11(13)
<b>DPDP·Br</b>	P(1)-N(1) : 1.6325(19) P(1)-N(2) : 1.6187(17) N(1)-H(1) : 0.8800(2) N(2)-H(2) : 0.8800(1)	N(1)-P(1)-N(2) : 109.19(9) N(1)-P(1)-C(11) : 113.45(8) N(1)-P(1)-C(21) : 106.70(8) N(2)-P(1)-C(11) : 108.83(8) N(2)-P(1)-C(21) : 111.61(9)
<b>DPDP·I (PM1)</b>	P(1)-N(1) : 1.6162(26) P(1)-N(2) : 1.6271(22) N(1)-H(1) : 0.8801(23) N(2)-H(2) : 0.8803(25)	N(1)-P(1)-N(2) : 120.554(132) N(1)-P(1)-C(11) : 103.272(91) N(1)-P(1)-C(21) : 107.498(110) N(2)-P(1)-C(11) : 108.838(113) N(2)-P(1)-C(21) : 106.097(103)
<b>DPDP·I (PM2)</b>	P(1)-N(1) : 1.619(4) P(1)-N(2) : 1.617(4) P(2)-N(3) : 1.616(4) P(2)-N(4) : 1.621(4) N(1)-H(1) : 0.8799(30) N(2)-H(2) : 0.8800(37) N(3)-H(3) : 0.8800(32) N(4)-H(4) : 0.8799(31)	N(1)-P(1)-N(2) : 108.2(2) N(3)-P(2)-N(4) : 110.7(2) N(1)-P(1)-C(1P) : 107.64(18) N(1)-P(1)-C(7P) : 113.17(19) N(2)-P(1)-C(1P) : 114.27(19) N(2)-P(1)-C(7P) : 105.57(17) N(3)-P(2)-C(13P) : 106.28(17) N(3)-P(2)-C(19P) : 112.93(18) N(4)-P(2)-C(13P) : 112.28(17) N(4)-P(2)-C(19P) : 106.23(18)

**Table S3.** Hydrogen bond data for DPDP·Cl, DPDP·Br and DPDP·I (PM1 & PM2)

Compound	D-H...A	d(D-H)	d(H...A)	d(D-A)	<DHA	Symmetry operations
<b>DPDP·Cl</b>	N(1)-H(1)...Cl(1) N(2)-H(2)...Cl(1)	0.8800(1) 0.8800(1)	2.4248(3) 2.4684(4)	3.228(3) 3.176(3)	152.007(11) 137.856(10)	-x+3/2, y+1/2, z-1/2 x, y, z
<b>DPDP·Br</b>	N(1)-H(1)...Br(1) N(2)-H(2)...Br(2)	0.8800(2) 0.8800(1)	2.6015(5) 2.5247(4)	3.2986(18) 3.3337(18)	136.826(13) 153.126(14)	x, y, z -x+1/2, y-1/2, z+1/2
<b>DPDP·I (PM1)</b>	N(1)-H(1)...I(1) N(2)-H(2)...I(1)	0.8801(23) 0.8803(25)	2.9376(4) 3.0933(3)	3.7496(26) 3.8534(25)	154.204(144) 145.822(163)	x, y, z x-1/2, y-1/2, z
<b>DPDP·I (PM2)</b>	N(1)-H(1)...I(1) N(2)-H(2)...I(1) N(3)-H(3)...I(2) N(4)-H(4)...I(2)	0.8799(30) 0.8800(37) 0.8800(32) 0.8799(31)	2.9785(30) 2.8188(27) 2.8188(25) 3.1277(22)	3.691(5) 3.566(5) 3.586(4) 3.939(5)	139.386(206) 143.6780(258) 146.7033(203) 154.2955(213)	x-1, y, z x, y, z x, y, z+1 -x+1, y+1/2, -z+1

**Table S4.** Selected torsion and bond angles [°] involved in hydrogen bonding for DPDP·Cl, DPDP·Br and DPDP·I (PM1 & PM2)

Compound	Torsion angle and Bond angle
<b>DPDP·Cl</b>	P(1)-N(1)-H(1)-Cl(1) : 134.858(18) P(1)-N(2)-H(2)-Cl(1) : 96.745(16) N(1)-Cl(1)-N(2) : 140.699(4)
<b>DPDP·Br</b>	P(1)-N(1)-H(1)-Br(1) : -95.882(20) P(1)-N(2)-H(2)-Br(1) : 137.398(25) N(1)-Br(1)-N(2) : 140.856(4)
<b>DPDP·I (PM1)</b>	P(1)-N(1)-H(1)-I(1) : -115.030(294) P(1)-N(2)-H(2)-I(1) : -118.607(16) N(1)-I(1)-N(2) : 137.605 (49)
<b>DPDP·I (PM2)</b>	P(1)-N(1)-H(1)-I(1) : 120.696 (282) P(1)-N(2)-H(2)-I(1) : 114.769(354) N(1)-I(1)-N(2) : 153.953(81) P(2)-N(3)-H(3)-I(2) : 97.256(461) P(2)-N(4)-H(4)-I(2) : 134.657(442) N(1)-I(1)-N(2) : 114.354 (83)

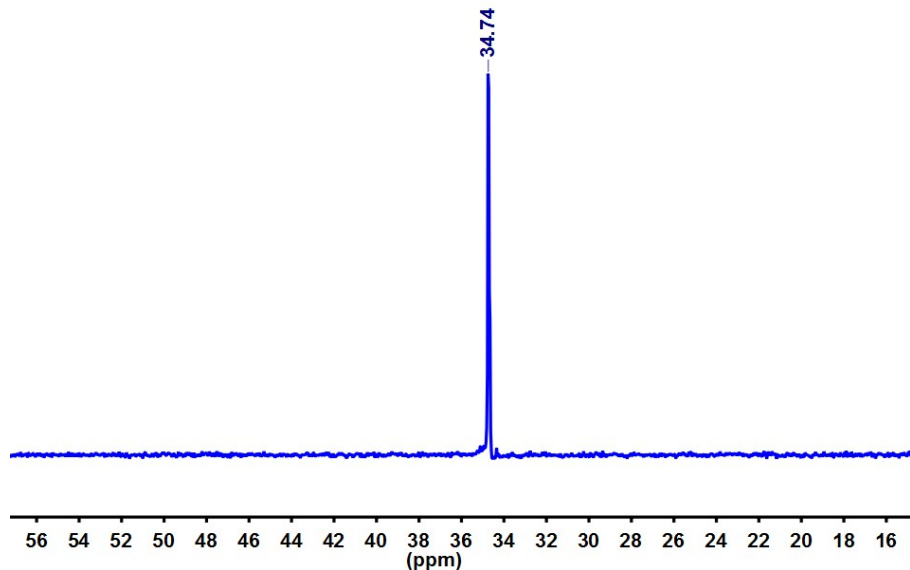


**Figure S1.**  $^{31}\text{P}$  NMR spectrum of DPDP·Cl

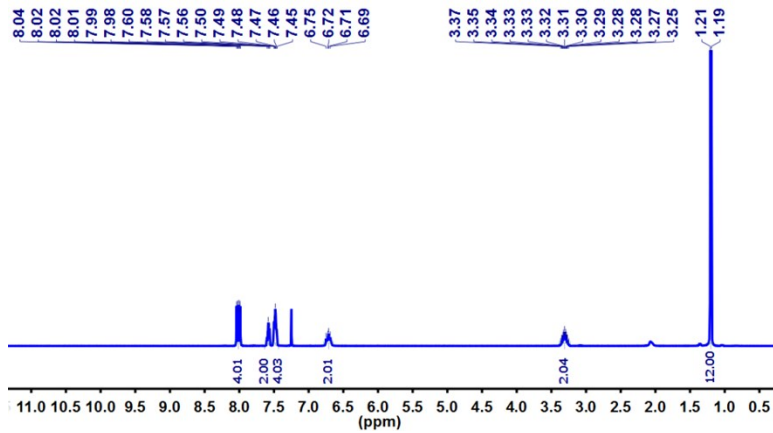


**Figure S2.** <sup>1</sup>H NMR spectrum of DPDP·Cl

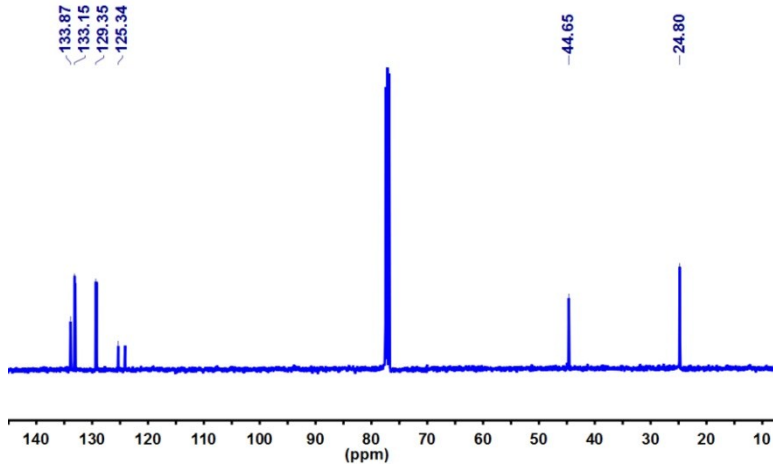


**Figure S3.** <sup>13</sup>C NMR spectrum of DPDP·Cl

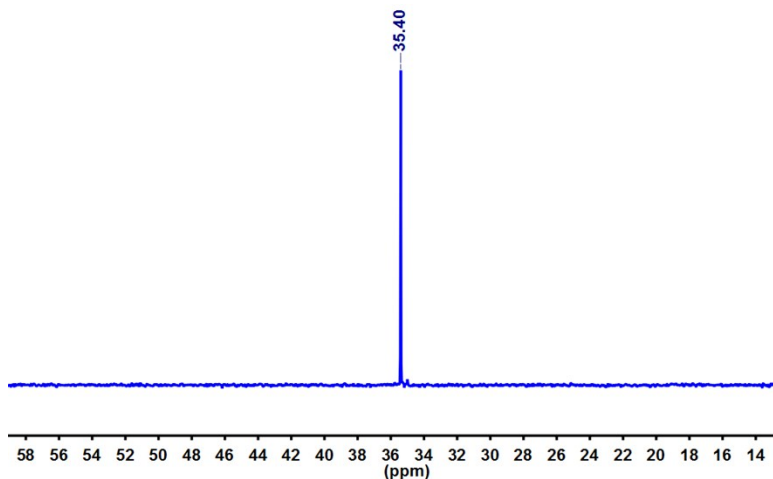


**Figure S4.** <sup>31</sup>P NMR spectrum of DPDP·I (PM1)

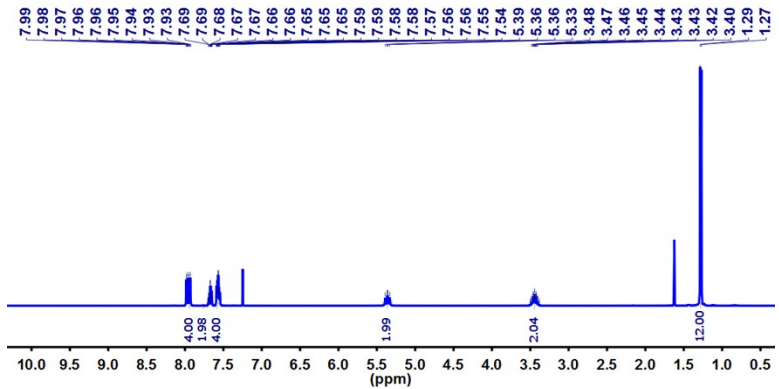


**Figure S5.**  $^1\text{H}$  NMR spectrum of DPDP-I (PM1)

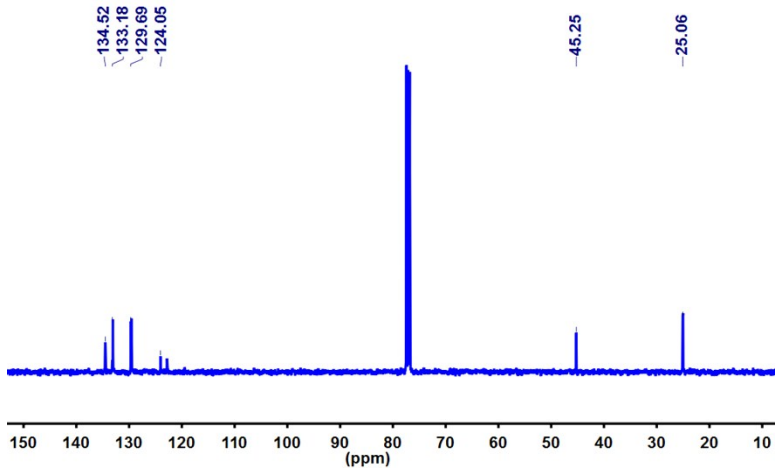


**Figure S6.**  $^{13}\text{C}$  NMR spectrum of DPDP-I (PM1)

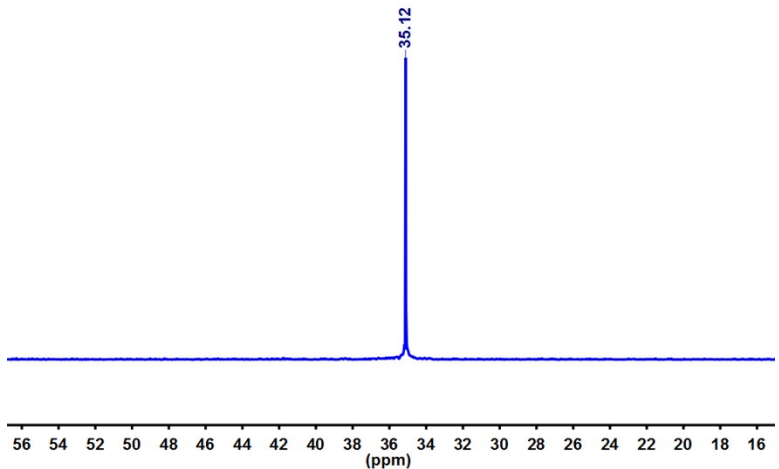


**Figure S7.**  $^{31}\text{P}$  NMR spectrum of DPDP-I (PM2)

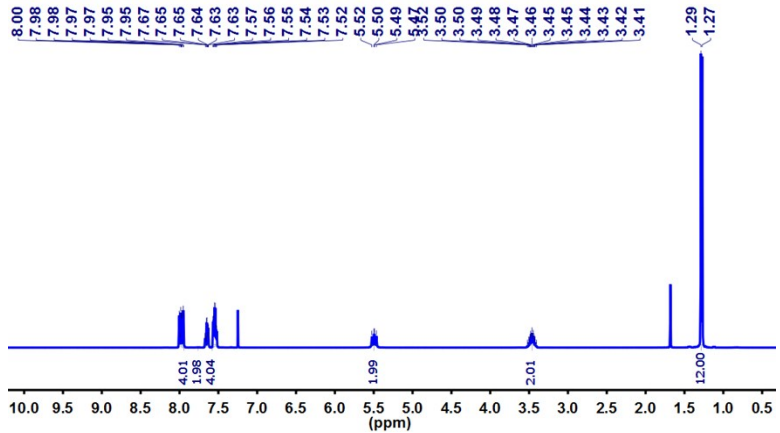


**Figure S8.**  $^1\text{H}$  NMR spectrum of DPDP·I (PM2)

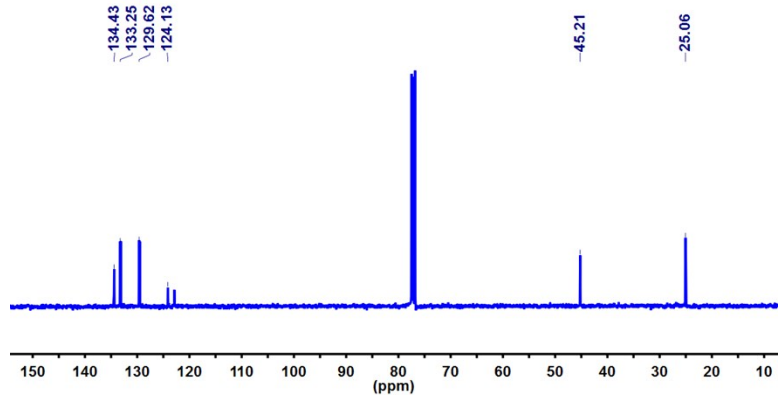


**Figure S9.**  $^{13}\text{C}$  NMR spectrum of DPDP·I (PM2)

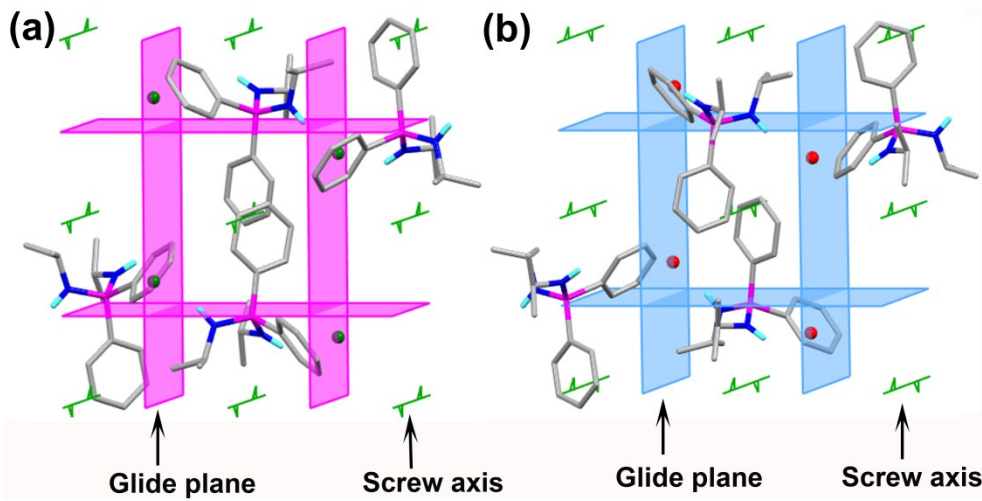


**Figure S10.** Crystal packing diagram for (a) DPDP·Cl and (b) DPDP·Br in the orthorhombic space group  $Pna2_1$

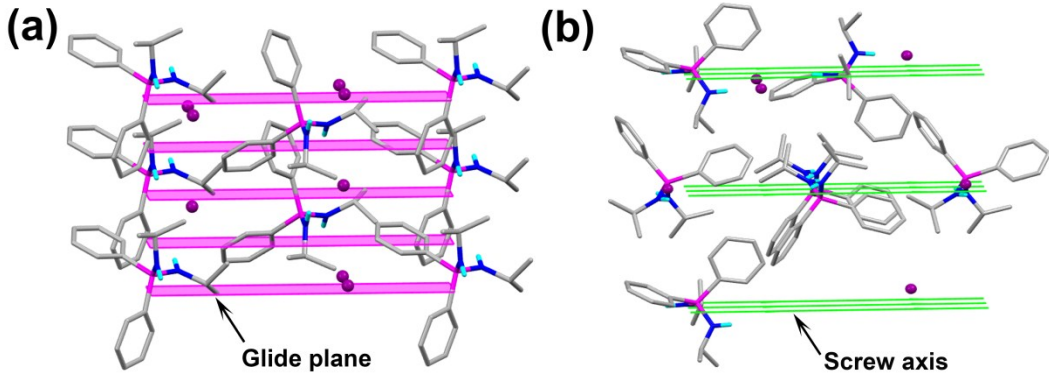


**Figure S11.** Crystal packing diagram for (a) DPDP·I (PM1) and (b) DPDP·I (PM2) in the monoclinic space group (a)  $Cc$  and (b)  $P2_1$

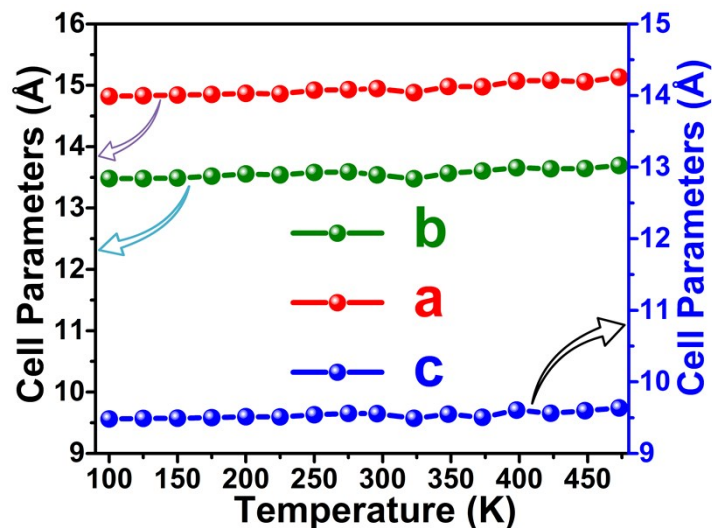


**Figure S12.** Variable temperature unit-cell parameters for DPDP·Cl

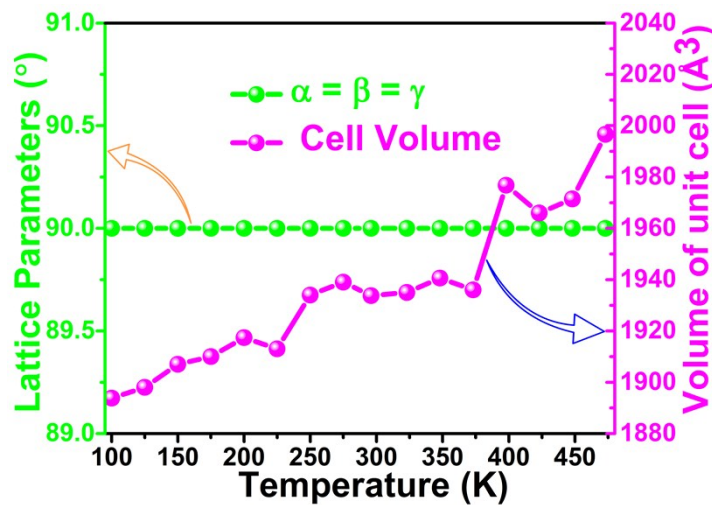


**Figure S13.** Variable temperature unit-cell parameters for DPDP·Cl

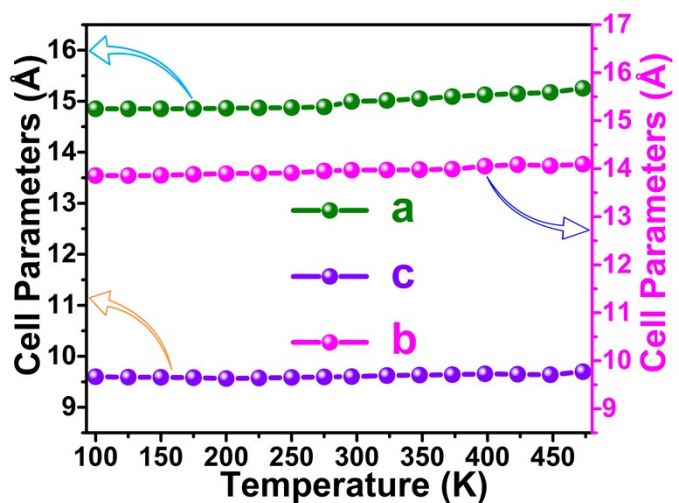


Figure S14. Variable temperature unit-cell parameters for DPDPhBr

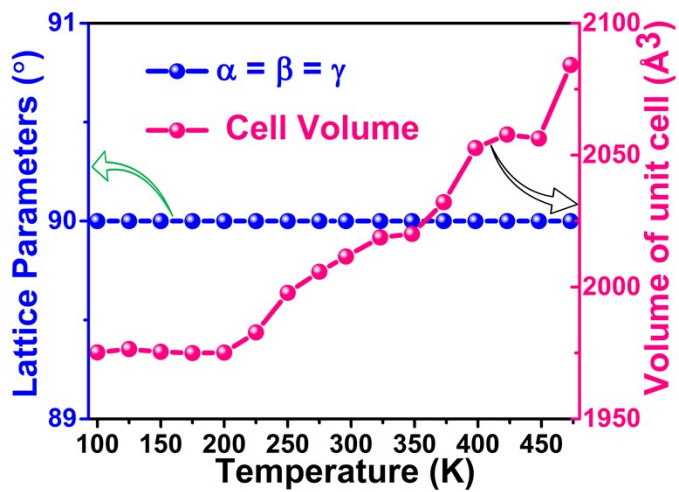


Figure S15. Variable temperature unit-cell parameters for DPDPhBr

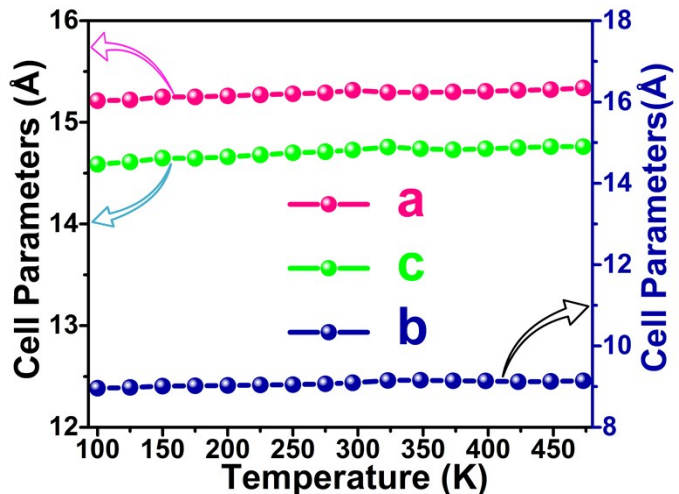


Figure S16. Variable temperature unit-cell parameters for DPDPhI (PM1)

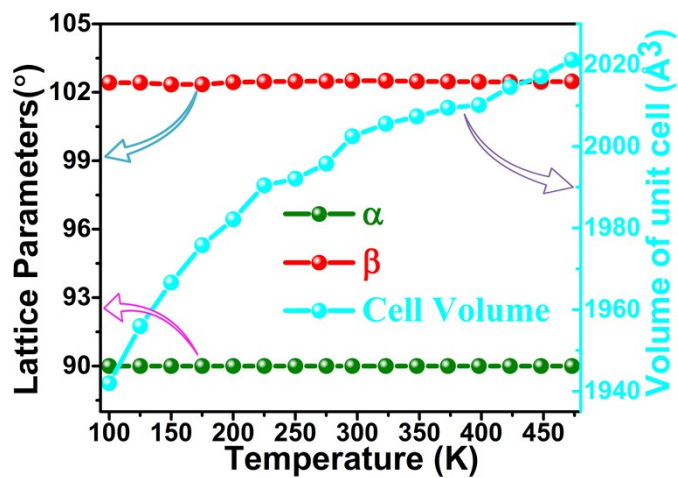


Figure S17. Variable temperature unit-cell parameters for DPDPI (PM1)

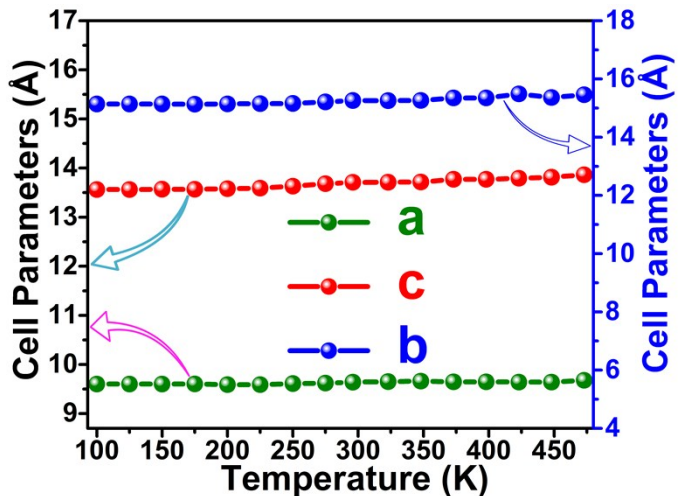


Figure S18. Variable temperature unit-cell parameters for DPDPI (PM2)

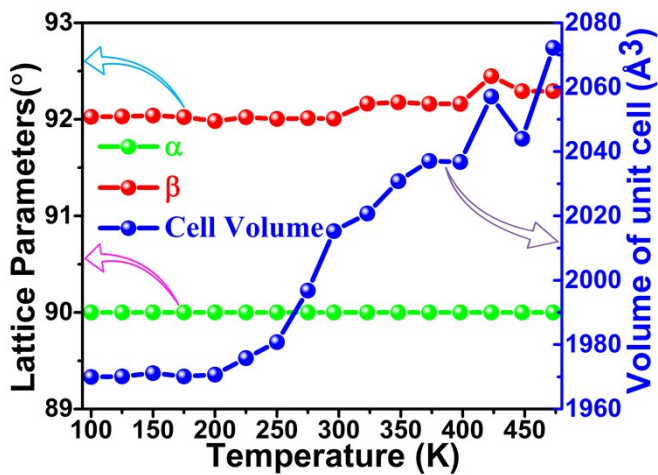


Figure S19. Variable temperature unit-cell parameters for DPDPI (PM2)

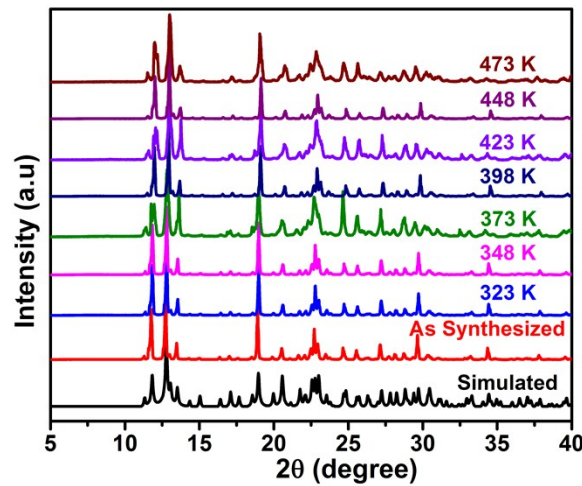


Figure S20. Variable temperature powder pattern for DPDP·Cl

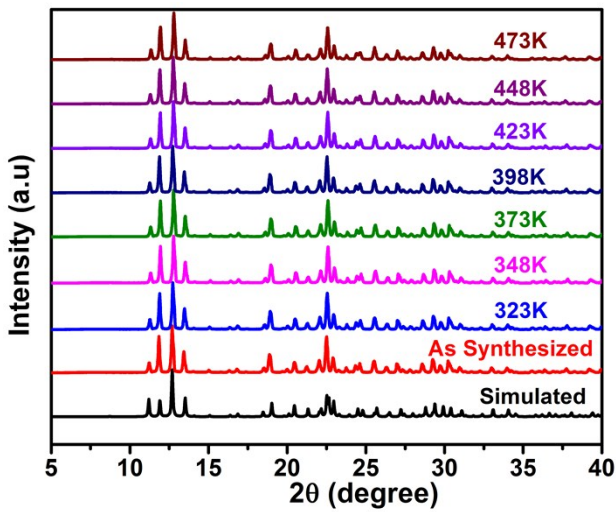


Figure S21. Variable temperature powder pattern for DPDP·Br

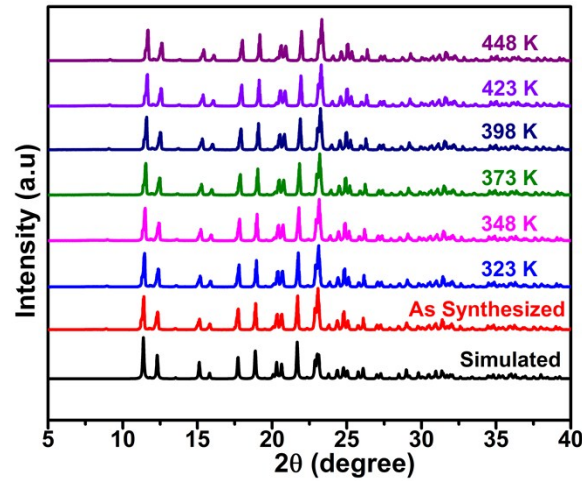


Figure S22. Variable temperature powder pattern for DPDP·I (PM1)

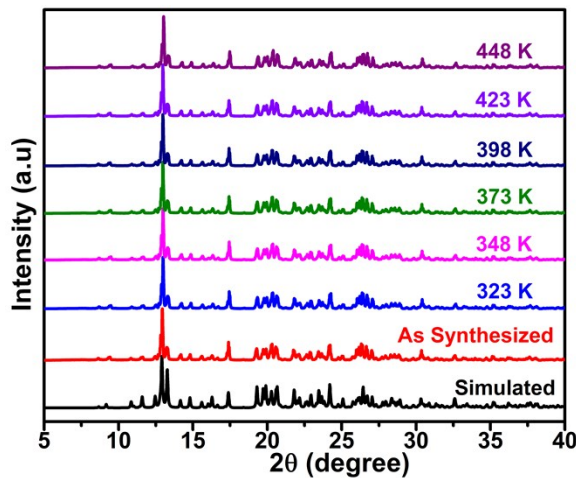


Figure S23. Variable temperature powder pattern for DPDP·I (PM2)

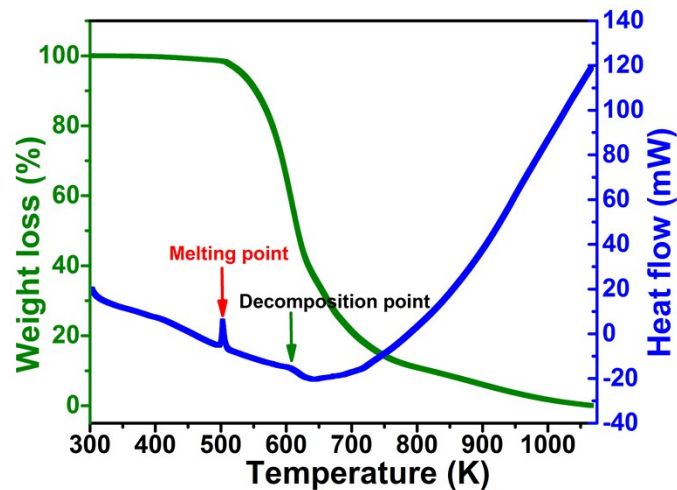


Figure S24. TGA and DTA analysis for DPDP·Cl

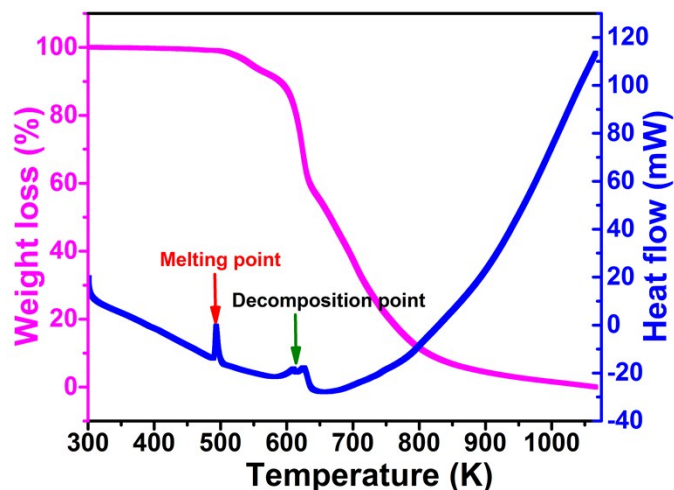
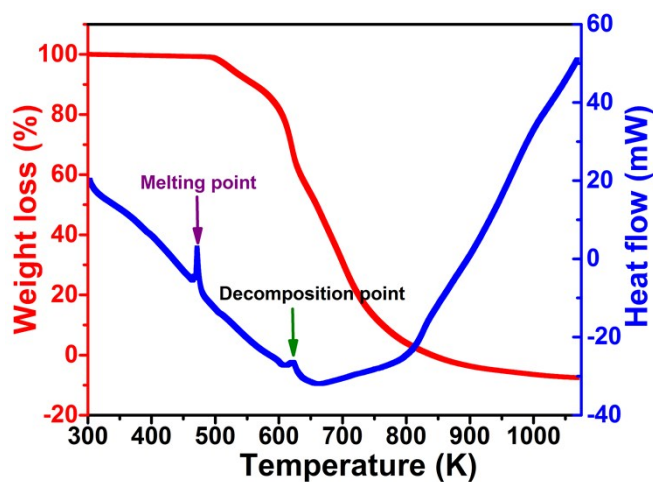
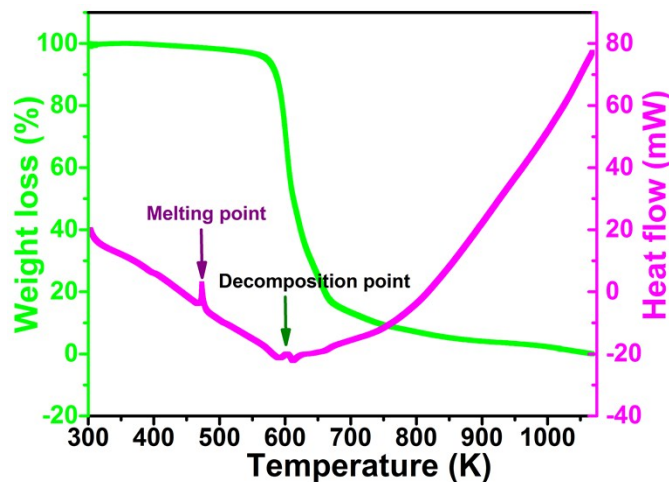


Figure S25. TGA and DTA analysis for DPDP·Br



**Figure S26.** TGA and DTA analysis for DPDP-I (PM1)



**Figure S27.** TGA and DTA analysis of DPDP-I (PM2)

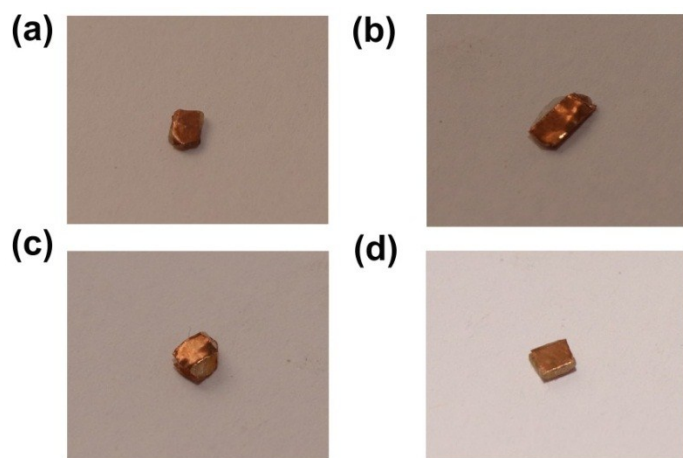


**Figure S28.** The photo of the measured crystals for (a) DPDP-Cl, (b) DPDP-Br, (c) DPDP-I (PM1) and DPDP-I (PM2)

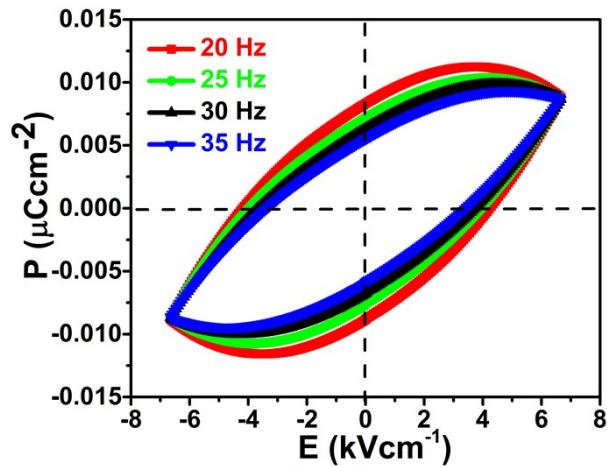


**Figure S29.** Frequency dependent P-E hysteresis loops for DPDP·Cl

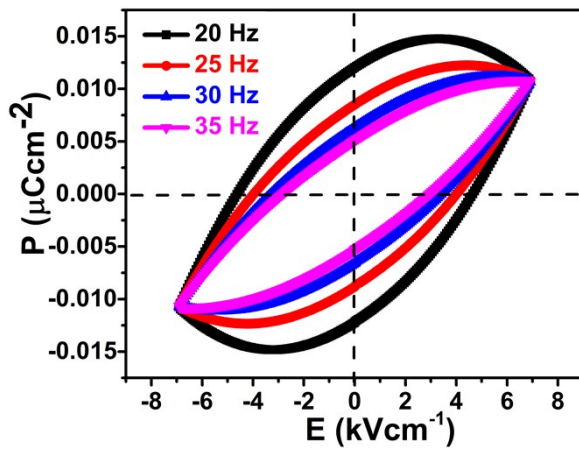


**Figure S30.** Frequency dependent P-E hysteresis loops for DPDP·Br

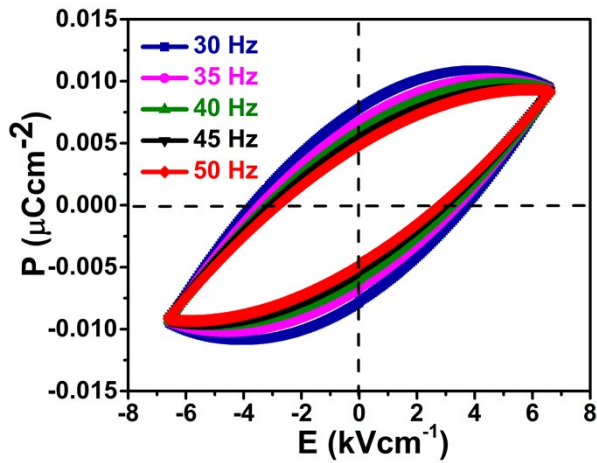


**Figure S31.** Frequency dependent P-E hysteresis loops for DPDP·I (PM1)

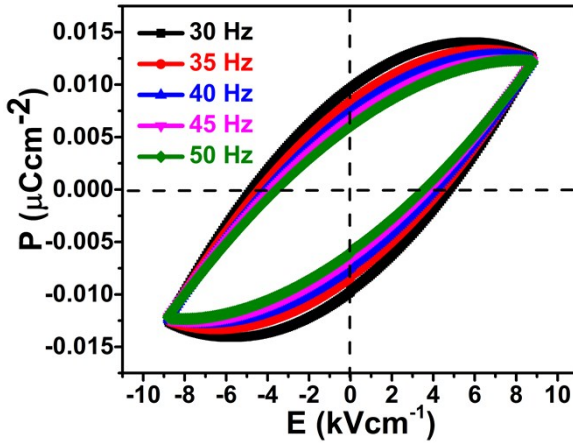


**Figure S32.** Frequency dependent P-E hysteresis loops for DPDP-I (PM2)

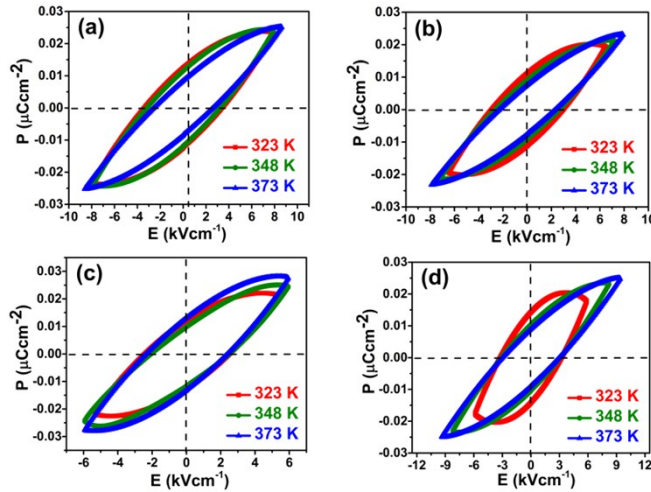


**Figure S33.** Temperature dependent P-E hysteresis loops for (a) DPDP-Cl, (b) DPDP-Br, (c) DPDP-I (PM1) and (d) DPDP-I (PM2)

**Table S5.** The observed spontaneous ( $P_s$ ), remanent polarization ( $P_r$ ) and coercive field ( $E_c$ ) of all the ferroelectric materials at a frequency of 30 Hz

S.No	Ferroelectric Materials	P-E loop measured direction	Area (mm <sup>2</sup> )	Thickness (nm)	Temperature (K)	$P_s$ (μCcm <sup>-2</sup> )	$P_r$ (μCcm <sup>-2</sup> )	$E_c$ (kVcm <sup>-1</sup> )
1	DPDP-Cl	'b' axis	9.3744	1e <sup>6</sup>	296	0.0089	0.0064	3.73
					323	0.0236	0.0137	3.45
					348	0.0239	0.0130	3.26
					373	0.0253	0.0101	2.64
2	DPDP-Br	'b' axis	19.864	0.71e <sup>6</sup>	296	0.0108	0.0062	3.39
					323	0.0194	0.0110	3.01
					348	0.0213	0.0092	2.59
					373	0.0232	0.0076	2.29
3	DPDP-I (PM1)	'b' axis	5.4272	1.15e <sup>6</sup>	296	0.0095	0.0078	3.70
					323	0.0208	0.0121	2.56
					348	0.0243	0.0101	2.48
					373	0.0278	0.0131	2.35
4	DPDP-I (PM2)	'b' axis	5.304	0.71e <sup>6</sup>	296	0.0127	0.0097	4.75
					323	0.0177	0.0143	3.27
					348	0.0232	0.0160	3.04
					373	0.0248	0.0090	2.89

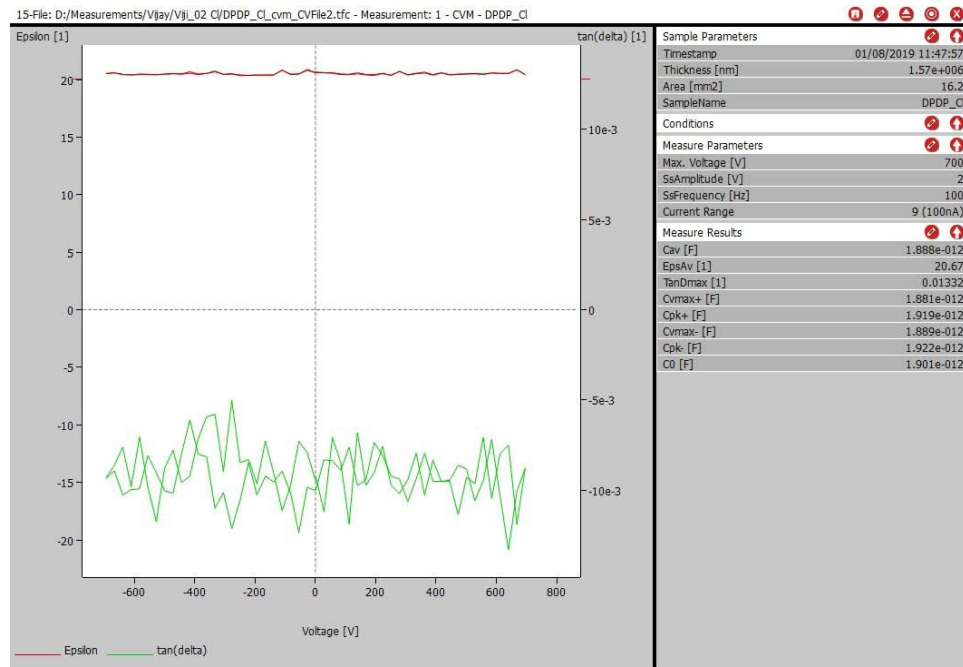


**Figure S34.** Electric field dependent dielectric constant of DPDP·Cl

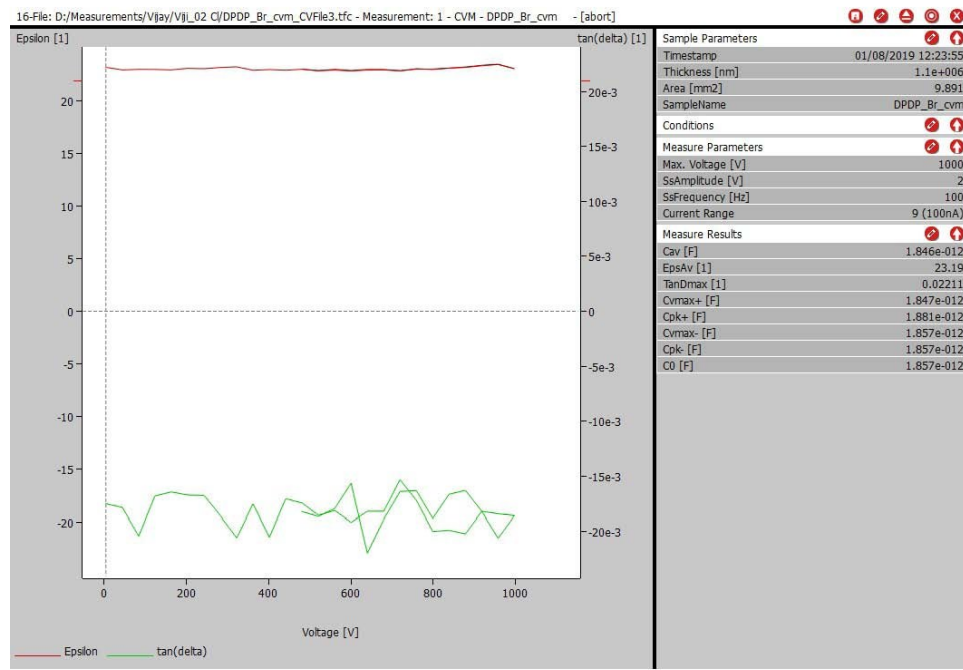


**Figure S35.** Electric field dependent dielectric constant of DPDP·Br

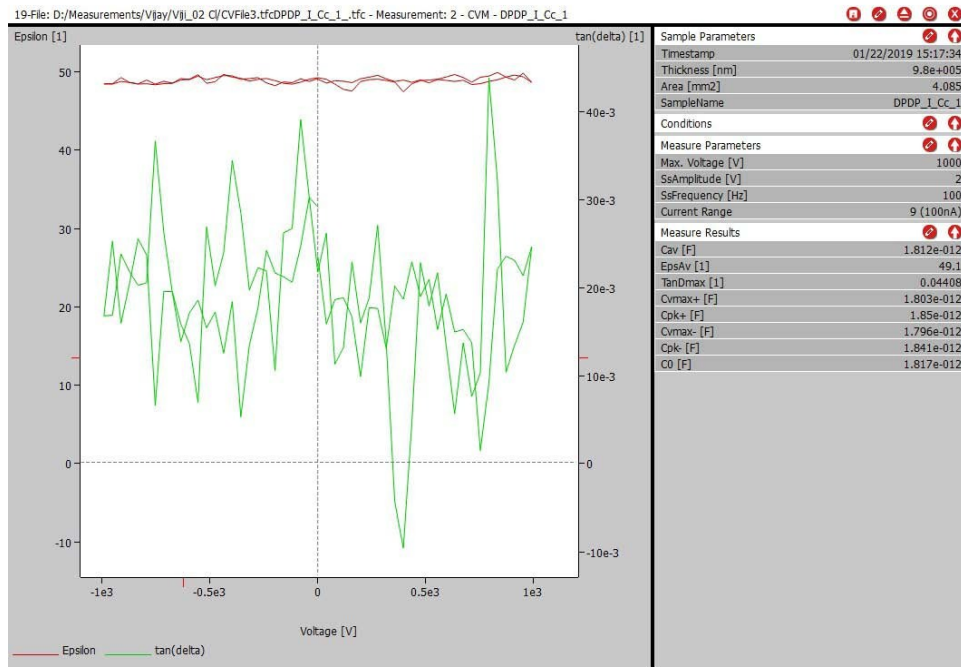


**Figure S36.** Electric field dependent dielectric constant of DPDP-I (PM1)

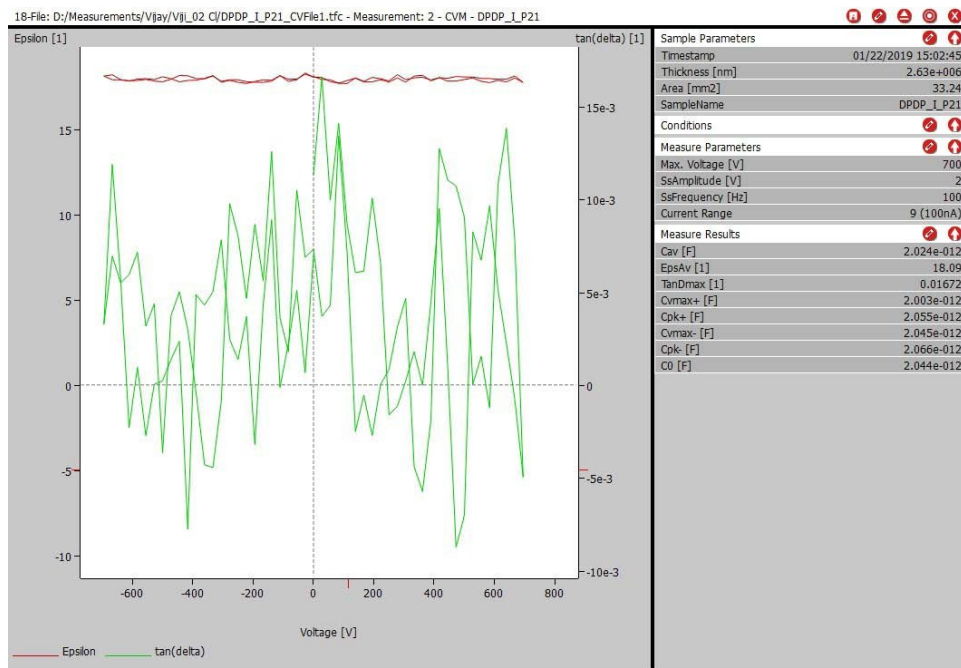


**Figure S37.** Electric field dependent dielectric constant of DPDP-I (PM2)

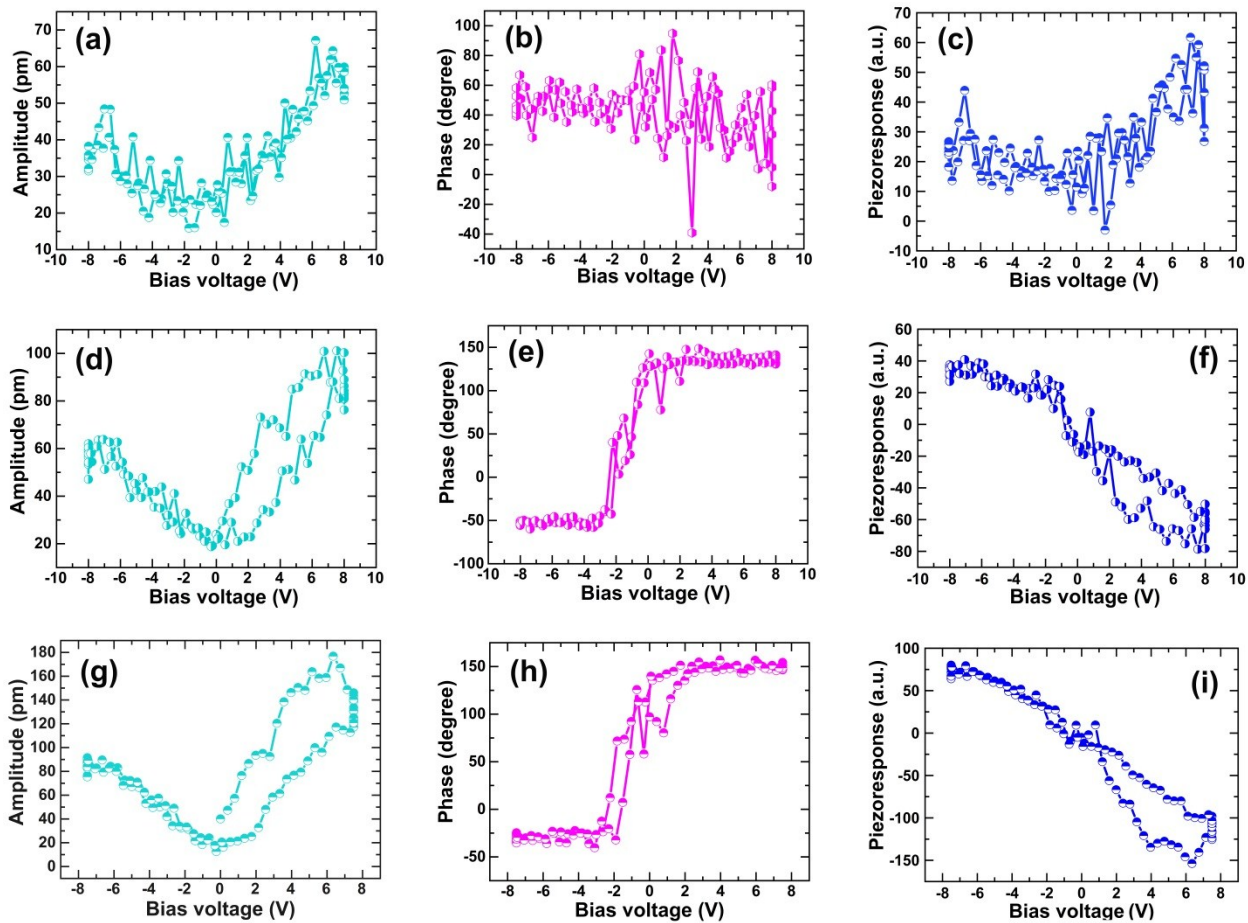


**Figure S38.** The room temperature V-PFM analysis for DPDPCl (a,b,c), DPDPBr (d,e,f) and DPDI (PM1) (g,h,i) showing (a, d, g) amplitude-voltage loops, (b, e, h) phase- voltage loops and (c, f, g) piezoresponse loops.

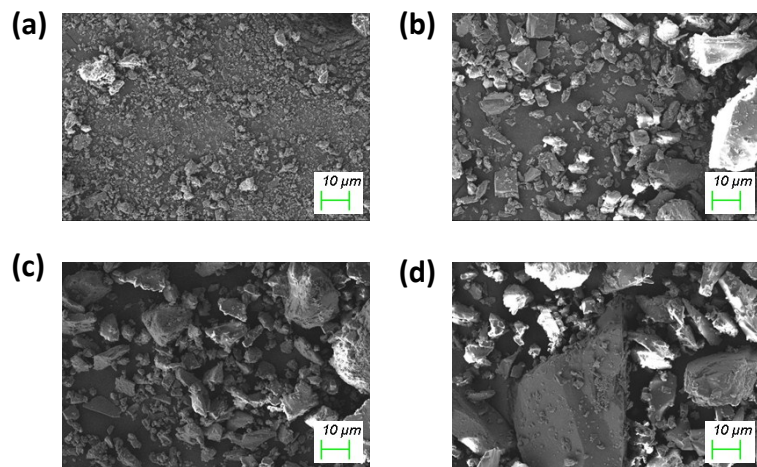


**Figure S39.** Scanning electron microscopy (SEM) images of (a) DPDPCl, (b) DPDPBr, (c) DPDI (PM1) and (d) DPDI (PM2)

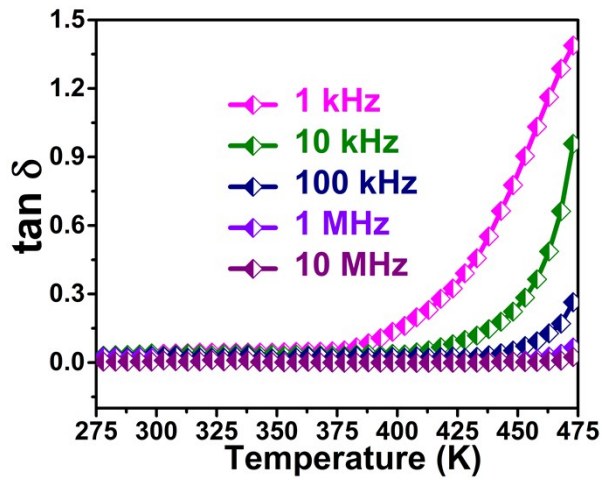


**Figure S40.** Temperature dependent dielectric loss of DPDPCl at various frequencies

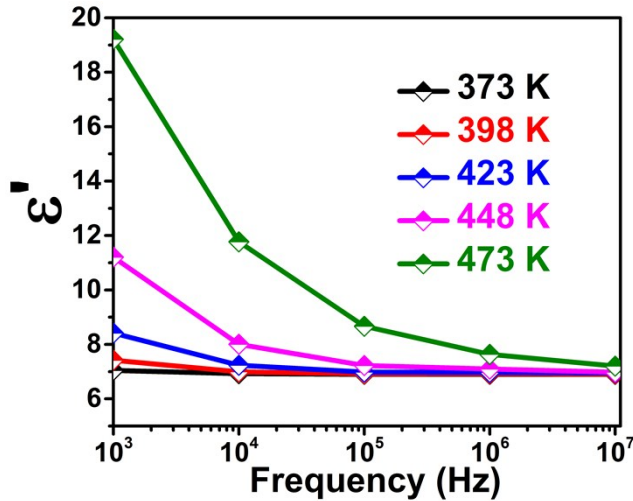


**Figure S41.** Frequency dependent dielectric constant of DPDPCl at different temperatures

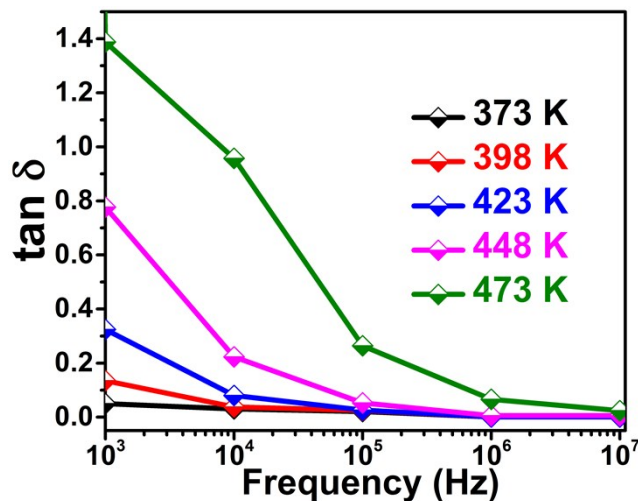


**Figure S42.** Frequency dependent dielectric loss of DPDPCl at different temperatures

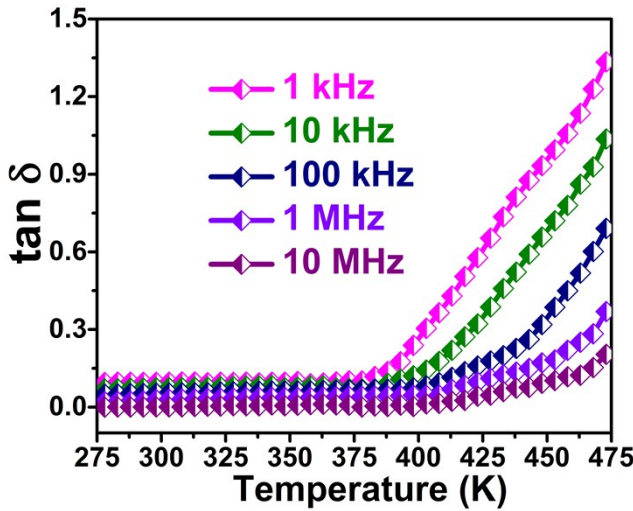


Figure S43. Temperature dependent dielectric loss of DPDP·Br at various frequencies

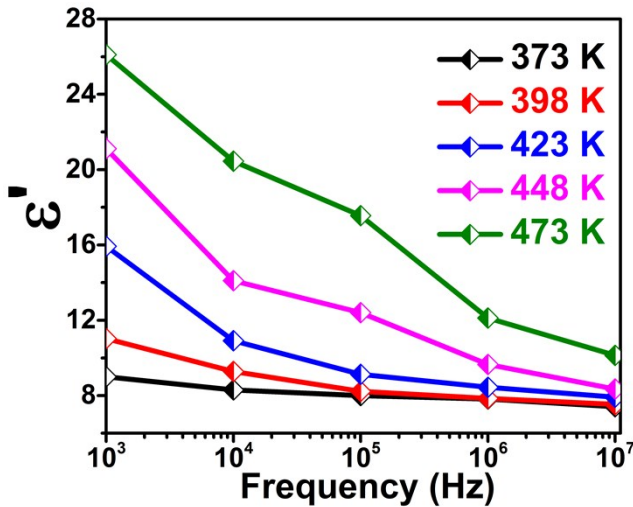


Figure S44. Frequency dependent dielectric constant of DPDP·Br at different temperatures

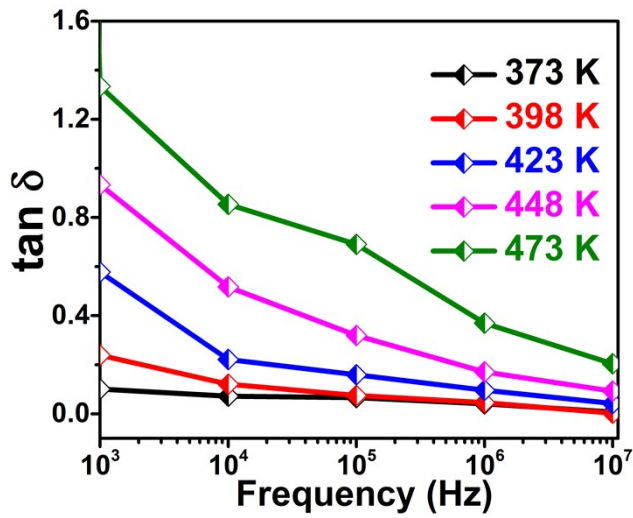
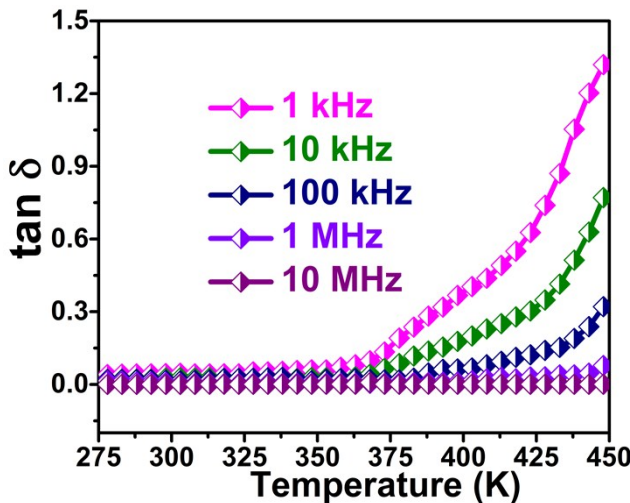
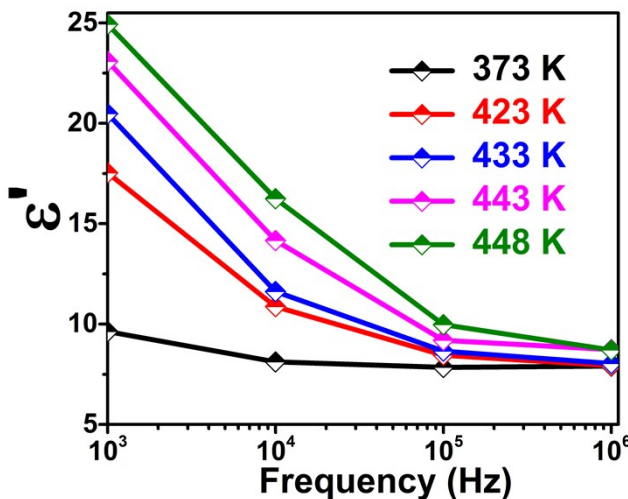


Figure S45. Frequency dependent dielectric loss of DPDP·Br at different temperatures



**Figure S46.** Temperature dependent dielectric loss of DPDPI (PM1) at various frequencies



**Figure S47.** Frequency dependent dielectric constant of DPDPI (PM1) at different temperatures

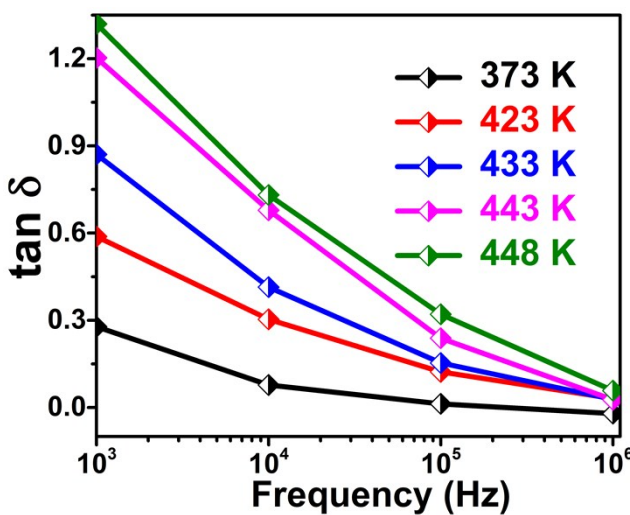


**Figure S48.** Frequency dependent dielectric loss of DPDPI (PM1) at different temperatures

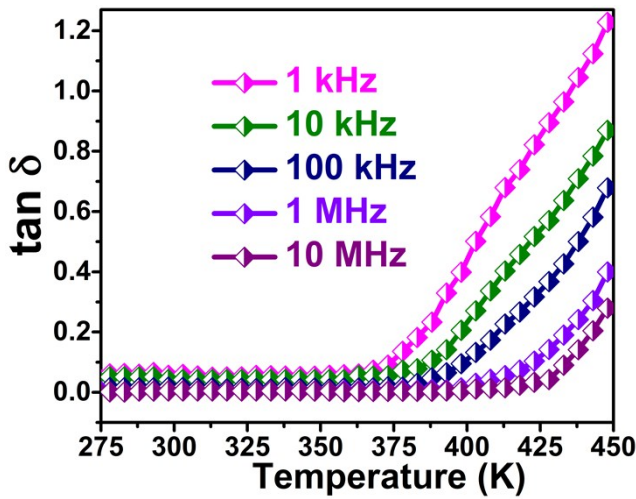


**Figure S49.** Temperature dependent dielectric loss of DPDPI (PM2) at various frequencies

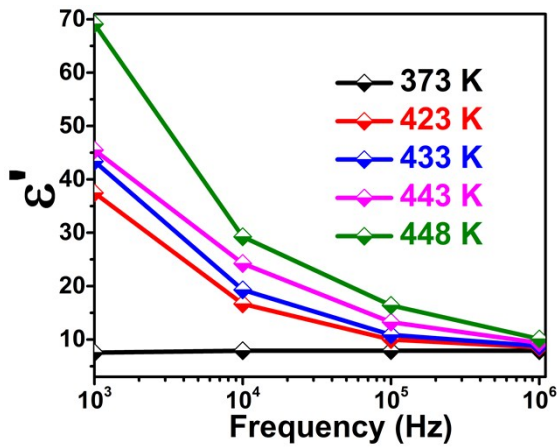


**Figure S50.** Frequency dependent dielectric constant of DPDPI (PM2) at different temperatures

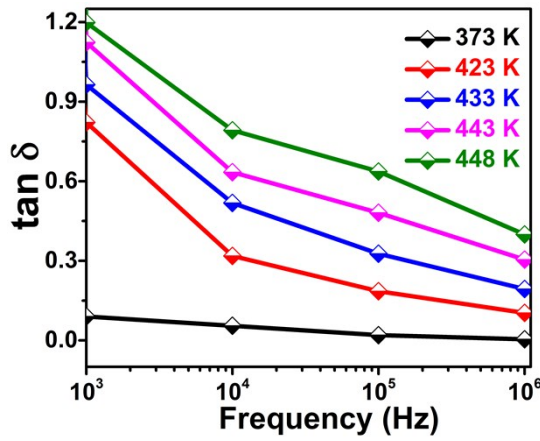


**Figure S51.** Frequency dependent dielectric loss of DPDPI (PM2) at different temperatures

**Table S6.** Comparison of some of the known piezoelectric materials and phosphonium halides

S.No	Piezoelectric Materials	$d_{33}$ (pCN <sup>-1</sup> )	Reference
1	BaTiO <sub>3</sub> [001] (no poling)	10	6
2	LiNbO <sub>3</sub>	11	9
3	Croconic acid	5, 15	6, 10
4	DIPAB	11	6
5	Rochelle salt	7	8
6	Imidazolium periodate	4.2	7
7	DPDP·Cl	3	This work
8	DPDP·Br	4	This work
9	DPDP·I (PM1)	7	This work
10	DPDP·I (PM2)	8	This work

**Table S7.** Dipole moment calculation of all the phosphonium halides

S.No	Ferroelectric Materials	Dipole moment (Debye)
1	DPDP·Cl	17.33
2	DPDP·Br	17.97
3	DPDP·I (PM1)	21.29
4	DPDP·I (PM2)	69.14

**Table S8.** Frequency dependent dielectric constant calculation of DPDP·Cl, DPDP·Br, DPDP·I (PM1) and DPDP·I (PM2)

Compound	Frequency	Dielectric Constant
DPDP·Cl	100 Hz	57.21
	1 kHz	33.37
	10 kHz	31.23
	100 kHz	30.19
	1 MHz	29.4
DPDP·Br	100 Hz	92.29
	1 kHz	40.13
	10 kHz	39.12
	100 kHz	37.12
	1 MHz	37.02
DPDP·I(PM1)	100 Hz	217.83
	1 kHz	124.47
	10 kHz	115.14
	100 kHz	113.27
	1 MHz	111.72
DPDP·I(PM2)	100 Hz	275.36
	1 kHz	111.32
	10 kHz	108.39
	100 kHz	105.46
	1 MHz	102.53

## References

- (1) T. Vijayakanth, A. K. Srivastava, F. Ram, P. Kulkarni, Kadhiravan Shanmuganathan, B. Praveenkumar and R. Boomishankar, *Angew. Chem. Int. Ed.* 2018, **57**, 9054.
- (2) G. M. Sheldrick, *Acta Crystallogr.C* 2015, **71**, 3.
- (3) A.L. Spek, *Acta Cryst.* 2009, **D65**, 148.
- (4) X. Li, C. Chen, H. Deng, H. Zhang, D. Lin, X. Zhao and H. Luo, *Crystals* 2015, **5**, 172.
- (5) M. Frisch, G.Trucks, H. Schlegel, *GAUSSIAN 03, Revision B. 05, Gaussian, Inc., Wallingford, CT*, 2004.
- (6) Y. M. You, W. Q. Liao, D. Zhao, H. Y. Ye, Y. Zhang, Q. Zhou, X. Niu, J. Wang, P. F. Li, D. W. Fu, Z. Wang, S. Gao, K. Yang, J. Liu, J. Li, Y. Yan and R. G. Xiong, *Science* 2017, **357**, 306.
- (7) Y. Zhang, H. Y. Ye, H. L. Cai, D. W. Fu, Q. Ye, W. Zhang, Q. Zhou, J. Wang, G. L. Yuan and R. G. Xiong, *Adv. Mater.* 2014, **26**, 4515.
- (8) C. Wan and C. R. Bowen, *J. Mater. Chem. A* 2017, **5**, 3091.
- (9) Q. Pan, Z. B. Liu, H. Y. Zhang, W. Y. Zhang, Y. Y. Tang, Y. M. You, P. F. Li, W. Q. Liao, P. P. Shi, R. W. Ma, R. Y. Wei and R. G. Xiong, *Adv. Mater.* 2017, **29**, 1700831.
- (10) S. Horiuchi, J. Tsutsumi, K. Kobayashi, R. Kumai and S. Ishibashi, *J. Mater. Chem. C*, 2018, **6**, 4714.